Effect of Centerbody Scattering on Propeller Noise

Stewart A. L. Glegg*
Florida Atlantic University, Boca Raton, Florida 33431

This paper describes how the effect of acoustic scattering from the hub or centerbody of a propeller will affect the far-field noise levels. A simple correction to Gutin's formula for steady loading noise is given. This is a maximum for the lower harmonics but has a negligible effect on the higher frequency components that are important subjectively. The case of a blade vortex interaction is also considered, and centerbody scattering is shown to have a significant effect on the acoustic far field.

Introduction

PROPELLER noise prediction methods[1-4] currently assume that the rotor is operating in an acoustic free field and consequently overlook the effects of reflections from the fuselage of the aircraft or the engine and hub of the rotor. With larger hub-to-tip ratios being introduced on ATP propellers, the assumption that the rotor operates in a free field becomes questionable. In particular, the rotor hub and engine will act as a scattering object in the near field of the source and may either shield or amplify the acoustic radiation, depending on the position of the source relative to the observer. The purpose of this paper is to evaluate the importance of centerbody scattering on the sound radiation from highly loaded propellers. The theory is developed so that it may be incorporated directly into the classical description of propeller noise in the frequency domain.[1,2,4] The propeller is modeled acoustically by a point dipole source rotating in a circle of radius a, and the centerbody is represented by a cylinder of infinite length. This assumes that the load distribution on each blade may be represented by a point loading at a suitable spanwise location (often taken to be 80% of the blade span). However, more recent analyses of propeller noise[3,4] are not restricted by this assumption, and the theory presented here can be extended to include radial load distributions in a similar manner.

To demonstrate the importance of centerbody scattering, two specific examples are considered. First the case of a highly loaded propeller with steady blade loadings is evaluated. This problem was originally considered by Gutin,[1] and a simple correction to this formulation is derived that allows for centerbody scattering. The more important case, however, occurs when the propeller blades encounter a sudden change in load, for instance a blade vortex interaction. In the free field, this generates a very impulsive acoustic signature with a distinctive pulse shape. The modification of this pulse caused by the centerbody of the propeller is considered in detail, and significant effects are shown even for small hub-to-tip ratios.

Analysis

The propeller is modeled by a set of point forces that rotate with angular velocity Ω in a circle of radius a. The hub and engine are modeled by a cylinder of radius b whose axis coincides with the axis of rotation of the propeller (see Fig. 1). The field is defined in terms of cylindrical coordinates $r \equiv (r, \phi, z)$, with the propeller in the $z = 0$ plane and the observer at $r_0 = (r_0, \phi_0, z_0)$.

The acoustic field from an arbitrary load distribution $f(r, \tau)$ normal to a closed surface S is given by[5]:

$$p(r_0,t) = \int_{-T}^{T}\int_{S} f(r,\tau) \cdot \mathbf{grad}\,[G(r_0,t\,|\,r,\tau)]\,\mathrm{d}S\,\mathrm{d}\tau \qquad (1)$$

where $G(\ )$ is an arbitrary Green function. When there are no scattering objects present, the free-field Green function is used in this equation. However, when reflecting surfaces are significant, the Green function should be chosen so that it satisfies the same boundary conditions as the acoustic field. Hence Eq. (1) is suitable for the analysis of the problem illustrated in Fig. 1, providing that the correct Green function is chosen. This is most easily specified in the frequency domain, and so the Fourier transform of Eq. (1) is evaluated using

$$\tilde{p}(r_0,\omega) = \int_{-\infty}^{\infty} p(r_0,t)e^{i\omega t}\,\mathrm{d}t$$

Also note that the sources lie in the plane $z = 0$ and that the surface integral in Eq. (1) should strictly be evaluated on both sides of this plane. However, if $f(r, \tau)$ is replaced by the pressure jump across $z = 0$, such that $\Delta f(r, \tau) = f(r_+, \tau) + f(r_-, \tau)$, then the surface integral may be replaced by the integral over the planform Σ on which $z = 0$, giving, in the frequency domain,

$$\tilde{p}(r_0,\omega) = \int_{\Sigma} \Delta f(r,\omega) \cdot \mathbf{grad}\,[\,\tilde{G}(r_0\,|\,r)]\,\mathrm{d}\Sigma \qquad (2)$$

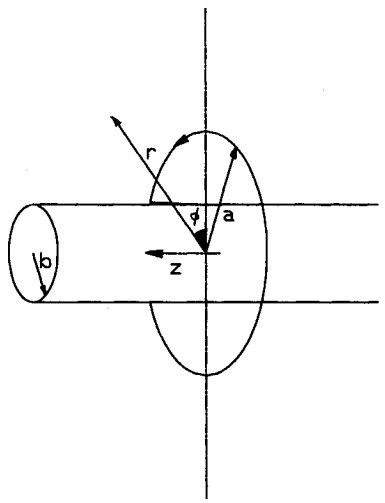

Fig. 1 Illustration of a ring source of radius a with a cylindrical centerbody of radius b. The point force F rotates with angular velocity Ω.

Received June 12, 1989; revision received Jan. 29, 1990.

*Associate Professor, Department of Ocean Engineering. Member AIAA.

The Green function may be defined as the sum of the free-field Green function, which describes the propagation of sound directly from the source to the observer in the absence of any scatters, and a complementary function, which specifies the scattered field. The sum of these must satisfy the rigid wall boundary condition on the surface of the cylinder

$$\frac{\partial \tilde{G}}{\partial r} = \frac{\partial}{\partial r}(\tilde{G}_0 + \tilde{G}_c) = 0 \qquad \text{on} \qquad r = b$$

The scattering of sound from a source near a cylinder is discussed in Refs. 6 and 7. These give the free-field Green function in cylindrical coordinates as

$$\tilde{G}_0(r_0|r) = \frac{i}{8\pi}\sum_{n=-\infty}^{\infty} e^{in(\phi_0-\phi)}\int_{-\infty}^{\infty} Z_n(\beta r, r_0)Z_n(\beta r_0, r)e^{i\alpha(z_0-z)}\,d\alpha$$

where $\beta = (k^2 - \alpha^2)^{1/2}$, $k = \omega/c_0$, and $Im(\beta) > 0$. The functions $Z_n(\ )$ are given by the Bessel functions

$$Z_n(\beta r, r_0) = \begin{cases} J_{|n|}(\beta r) & r_0 > r \\ H_{|n|}(\beta r) & r_0 < r \end{cases}$$

The scattered field may be specified using a similar series expansion of orthogonal functions in the form

$$\tilde{G}_c(r_0|r) = \frac{i}{8\pi}\sum_{n=-\infty}^{\infty} e^{in(\phi_0-\phi)}\int_{-\infty}^{\infty} A_{|n|}(\beta)Z_n(\beta r_0, 0)e^{i\alpha(z_0-z)}\,d\alpha$$

To satisfy the boundary condition on the surface of the cylinder, the coefficients $A_n(\beta)$ are defined for a source at $r = a$ as

$$A_n(\beta) = \frac{-J_n'(\beta b)H_n(\beta a)}{H_n'(\beta b)}$$

Each propeller blade is represented by a point force $F(\phi)$ that has a thrust component $L(\phi)$ in the axial direction and a drag component $D(\phi)$ in the azimuthal direction. Since $F(\phi)$ represents the force applied to the fluid, it can be defined in cylindrical coordinates as $F = (O,\ D,\ -L)$. If there are B propeller blades that rotate with angular velocity Ω, then the pressure jump at $z = 0$ is defined at any point $r \equiv (r,\ \phi,\ 0)$ by

$$\Delta f(r,\tau)\sum_{n=-\infty}^{\infty} F(\phi)\frac{1}{a}\delta(r-a)\delta\left(\phi - \Omega\tau + \frac{2\pi n}{B}\right)$$

By using Poisson's sum formula, this may be rewritten as

$$\Delta f(r,\tau) = \frac{BF(\phi)}{2\pi a}\delta(r-a)\sum_{m=-\infty}^{\infty} e^{imB(\phi-\Omega\tau)}$$

Then by taking the Fourier transform of this equation with respect to time and using Eq. (2), we obtain

$$\tilde{p}(r_0,\omega) = B\sum_m \int_{-\pi}^{\pi} F(\phi)\cdot \mathbf{grad}\,[\tilde{G}(r_0|r)]\,e^{imB\phi}\,d\phi\,\delta(\omega - mB\Omega) \tag{3}$$

Steady Loading Harmonics

For highly loaded propellers, the acoustic field is dominated by the steady loading noise. In this case, $F(\phi)$ is constant, so by substituting $\tilde{G} = \tilde{G}_0 + \tilde{G}_c$ into Eq. (3) and evaluating the integral over ϕ, we obtain

$$\tilde{p}(r_0,\omega) = \frac{-B}{4}\sum_m \int_{-\infty}^{\infty}\left(\alpha L - \frac{mBD}{a}\right)[Z_{mB}(\beta a, r_0)Z_{mB}(\beta r_0, a) + A_{|mB|}(\beta)Z_{mB}(\beta r_0, 0)]e^{imB\phi_0 + i\alpha z_0}\,d\alpha\,\delta(\omega - mB\Omega) \tag{4}$$

This integral may be evaluated using the method of stationary phase[6] in the region of the acoustic field where $kr_0 \gg mB$. As described in the appendix, an application of the stationary phase formula at the stationary point $\alpha = k\cos\theta_0$ and $\beta = k\sin\theta_0$, gives

$$\tilde{p}(r_0,\omega) = \frac{iB\Omega}{2R_0c_0}\sum_m mB\left(L\cos\theta_0 - \frac{D}{M}\right)[J_{mB}(ka\sin\theta_0) + A_{mB}(k\sin\theta_0)]e^{ikR_0 + imB\left(\phi_0 - \frac{\pi}{2}\right)}\,\delta(\omega - mB\Omega) \tag{5}$$

where $M = \Omega a/c_0$ and $R_0^2 = r_0^2 + z_0^2$. Here θ_0 represents the angle of the observer to the rotor axis.

This result corresponds to Gutin's formula for sound radiation from propellers, but here the effect of centerbody scattering is explicitly included by the addition of the term $A_{mB}(k\sin\theta_0)$. Consequently the level of each harmonic in the spectrum will be increased above the free-field level by a factor of

$$S_c = 1 + \frac{A_{mB}(k\sin\theta_0)}{J_{mB}(ka\sin\theta_0)}$$

where $k = mB\Omega/c_0$. For subsonic rotors, the functions $A_{mB}(\ )$ and J_{mB} may be approximated by their asymptotic forms for $ka \ll mB$, and the scattering correction factor simplifies to

$$S_c \simeq 1 + \left(\frac{b}{a}\right)^{2mB}\frac{1}{(kb\sin\theta_0)^2}$$

This shows that for larger values of mB the scattering effects are significantly reduced. Consequently only the lower harmonics will be affected by reflections from the hub or center-

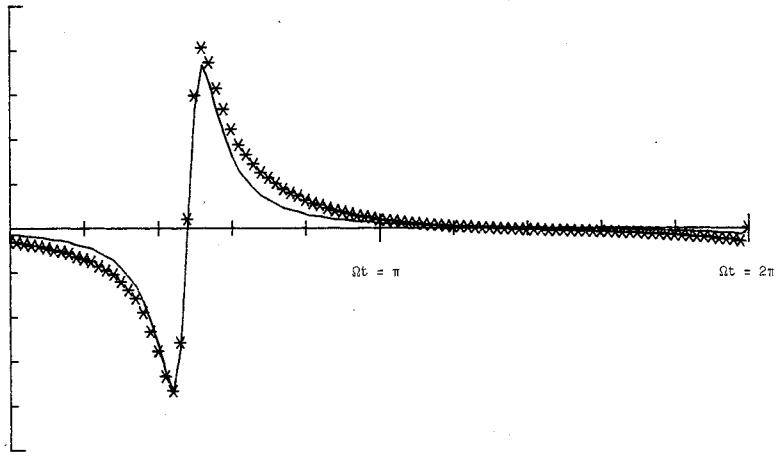

Fig. 2 The time history for one rotation of a single-bladed rotor both with and without centerbody scattering. Source Mach number $M = 0.7$, observer at $\theta_0 = 90$ deg, hub/tip ratio $b/a = 0.7$: —— no scattering, • • • • with scattering.

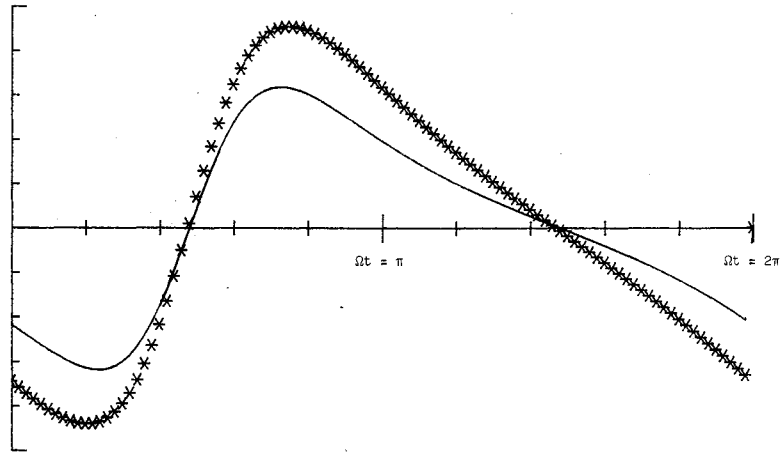

Fig. 3 The time history for one rotation of a single-bladed rotor both with and without centerbody scattering. Source Mach number $M = 0.7$, observer at $\theta_0 = 20$ deg, hub/tip ratio $b/a = 0.7$: —— no scattering, •••• with scattering.

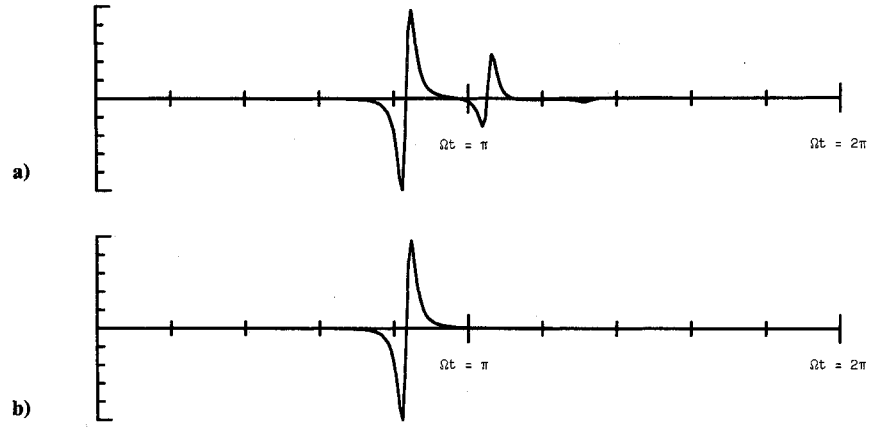

Fig. 4 The time histories for one rotation of a single-bladed rotor: a) with a centerbody present $b/a = 0.3$; b) without a centerbody. Source Mach number $M = 0.7$, observer at $\theta_0 = 45$ deg, and azimuth angle $\phi_0 = 0$ deg.

body of the propeller. This result also shows that reflections are more important for small values of θ_0 where the observer is closer to the axis of rotation.

By taking the inverse Fourier transform of Eq. (5), the time history in the acoustic field can be evaluated as

$$p(r_0,t) = \frac{B\Omega}{2\pi R_0 c_0}\left(L\cos\theta_0 - \frac{D}{M}\right)\sum_{m=1}^{\infty} mB\,|J_{mB}(ka\sin\theta_0) + A_{mB}(k\sin\theta_0)|\,\sin\left[mB\Omega\left(t-\frac{R_0}{c_0}\right) - mB\left(\phi_0 - \frac{\pi}{2}\right) - \gamma\right]$$

where $\gamma = \arg\,[J_{mB}(ka\sin\theta_0) + A_{mB}(k\sin\theta_0)]$.

This series has been evaluated for different positions in the acoustic field. Figures 2 and 3 show the time history for a single blade with a source Mach number $M = 0.7$ and a hub-to-tip ratio $b/a = 0.7$. At 90 deg to the axis of rotation (Fig. 2), the reflected field from the centerbody only introduces a small increase in the level of the positive going peak in the pressure time history. This increase is even less significant when b/a is reduced. However, at 20 deg to the axis (Fig. 3), the peak in the time history is significantly increased due to the centerbody scattering. In general, the results scale with $M\sin\theta_0$, and so scattering effects are more important at lower Mach numbers (in Fig. 3, $M\sin\theta_0 = 0.24$, and so a source moving with $M = 0.24$ would generate the same time histories as those shown in Fig. 3 at $\theta_0 = 90$ deg).

Perhaps one of the more interesting features of these results is the fact that the centerbody scattering does not alter the shape of the time history. Experimental observations of the two pulses shown in Fig. 3 would not indicate that scattering effects were important. However, a theoretical formulation that ignored the centerbody would underpredict the measured levels.

Unsteady Loading Noise

When the blade loading on the propeller varies rapidly with azimuthal location, the sound radiation will be dominated by unsteady loading effects. A particular example of this occurs for contrarotating propellers when a blade passes through a trailing vortex from the upstream rotor. In this case, there is a sharp change in blade loading, and a very impulsive acoustic signature is generated. The effect of centerbody scattering on this signature can be evaluated using the same approach as for the steady loads. However, in this case the blade loads will be a function of location ϕ and should be described using the Fourier series expansion

$$F(\phi) = \sum_{n=-\infty}^{\infty} F_n e^{in\phi}$$

where $F_n = (0, D_n, -L_n)$ represents the azimuthal harmonics of the blade loads. The acoustic time history is then evaluated as

$$p(r_0,t) = \frac{B\Omega}{2\pi R_0 c_0}\sum_{m=1}^{\infty} mB\,|C_{mB}|\,\sin\left[mB\Omega\left(t-\frac{R_0}{c_0}\right) - mB\left(\phi_0 - \frac{\pi}{2}\right) - \gamma\right]$$

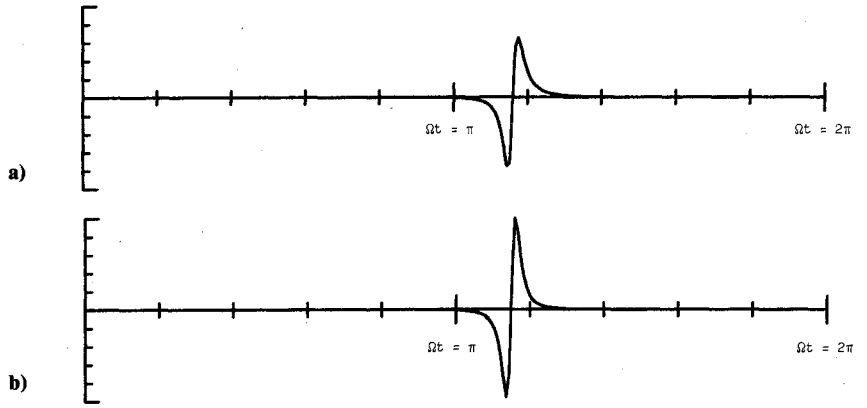

Fig. 5 The time histories for one rotation of a single-bladed rotor: a) with a centerbody present $b/a = 0.3$; b) without a centerbody. Source Mach number $M = 0.7$, observer at $\theta_0 = 45$ deg, and azimuth angle $\phi_0 = 180$ deg.

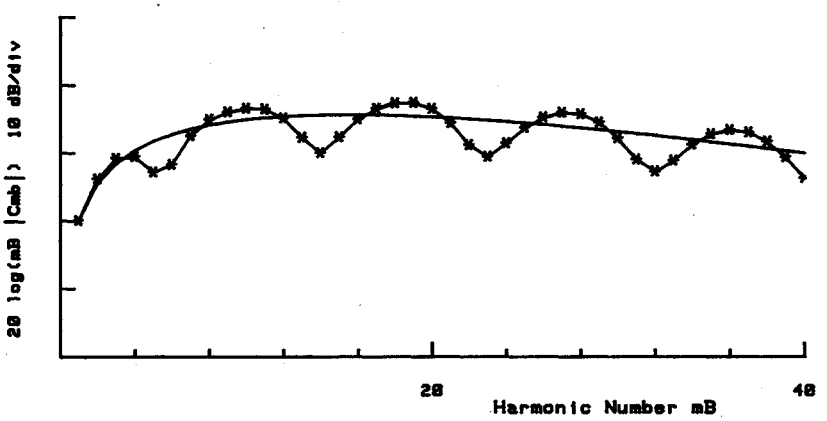

Fig. 6 The spectra of the time histories in Fig. 4. The curves show the peak amplitude of each harmonic: —— no scattering, -•- with scattering.

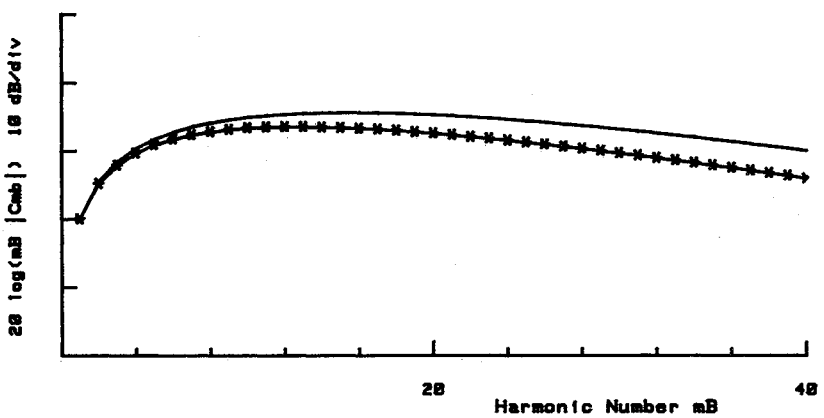

Fig. 7 The spectra of the time histories in Fig. 5. The curves show the peak amplitude of each harmonic: —— no scattering, -•- with scattering.

where $\gamma = \arg(C_{mB})$ and

$$C_{mB} = \sum_{n=-\infty}^{\infty} \left[L_n \cos\theta_0 - \frac{(mB+n)}{mB} D_n \right] [J_{mB+n}(ka \sin\theta_0) + A_{mB+n}(k \sin\theta_0)] e^{in(\phi_0 - \pi/2)}$$

To illustrate the importance of scattering for impulsive sources, this series has been evaluated using the blade loading function

$$F(\phi) = \frac{F_0}{1 + (\phi/\phi_s)^2}$$

with $\phi_s = 3.75$ deg, for a single bladed rotor, which represents an impulsive load when the blade passes through $\phi = 0$. The time histories in the acoustic far field are shown in Figs. 4 and 5 for observers at 45 deg to the rotor axis and a centerbody with radius $b/a = 0.3$. In Fig. 4 the observer is on the same side of the centerbody as the source ($\phi_0 = 0$ deg). This shows that both the acoustic free field and the field with the centerbody have a strong pulse of approximately the same level caused by the direct wave propagating from the source. However, when the centerbody is present, there is a second pulse of about half the magnitude of the first that represents the scattered field and arrives after the directly propagating pulse. In contrast, the time history for an observer at $\phi_0 = 180$ deg, (Fig. 5) which is directly opposite the source position, does not include the scattered pulse. The most important effect of the centerbody is to cause a slight reduction in the amplitude of the positive going peak.

The time histories in the plane of the rotor have also been considered, and it was found that the pulse shape was very sensitive to the observer azimuth angle ϕ_0. This is a consequence of the dipole nature of the acoustic source. However, in general there were no noticeable effects of centerbody scattering. In this case, the dipole directionality causes the acoustic field incident on the cylinder to be a minimum, and so the scattered field is minimal. The only exception to this observation occurred when $\phi_0 = 180$ deg, so that the source was completely shielded by the cylinder. At this location, the pulse shape is changing very rapidly with azimuth angle and has a significantly different shape from the pulse at other observer angles. When the centerbody is present, the peak level of the pulse was doubled, with very little change in shape.

The acoustic spectra of the pulses shown in Figs. 4 and 5 have also been computed and are shown in Figs. 6 and 7. The figures give 20 $\log_{10}(mB\,|C_{mB}|)$ as a function of harmonic number and represent the peak level of each harmonic in the acoustic spectrum. The effect of centerbody scattering is significant in the case when the observer lies on the same side of the cylinder as the impulsive source (Fig. 6), but relatively little effect is noticed when the source is shielded by the centerbody (Fig. 7). However, in the later case, the higher harmonics are reduced by 4 dB.

Conclusion

This paper has considered the effect of centerbody scattering on the sound radiation from propellers. It has been shown that scattering may be significant for the lower harmonics of a highly loaded propeller if the hub-to-tip ratio b/a is sufficiently large. In this case the effects of scattering scale with $M \sin\theta_0$, where M is the source Mach number, and are most important for low-speed applications when the observer is close to the axis of rotation. The shape of the time history generated by the blade is not affected by reflections, but its magnitude will be increased.

When the acoustic signature is impulsive, then centerbody scattering becomes important at lower hub-to-tip ratios. The examples considered here for a hub-to-tip ratio $b/a = 0.3$ indicate the presence of a reflected pulse caused by the centerbody that is approximately half the amplitude of the directly propagating pulse when the observer lies on the same side of the centerbody as the source generating mechanism. When the acoustic source is shielded by the centerbody, the reflected pulse is eliminated, and a small change in the peak levels of the acoustic signature occurs.

The main conclusion of this paper is that centerbody scattering effects are small for steady loading noise from propellers but cannot be ignored for impulsive noise sources such as blade vortex interactions.

Appendix: Stationary Phase Evaluation of the Far-Field Equation

The far-field approximation of Eq. (4) may be obtained by using the method of stationary phase. Since the integrand tends to zero as $(a/r_0)^{mB}$ for small or imaginary values of β, the main contribution to the integral comes from the range of α where the functions $Z_n(\beta r_0, a)$ and $Z_n(\beta r_0, 0)$ are oscillatory. In this range, they may be replaced by their asymptotic forms for $r_0 > a$:

$$Z_n(\beta r_0,a) \simeq Z_n(\beta r_0,0) \simeq \sqrt{\frac{2}{\pi\beta r_0}}\, ei\left(\beta r_0 - \frac{|n|\pi}{2} - \frac{\pi}{4}\right)$$

and the integral of Eq. (4) may be reduced to the form

$$\tilde{p}(r_0,\omega) = -\frac{B}{4}\sum_n \int_{-\infty}^{\infty} f_n(\zeta)\, e^{ikR_0\phi_e(\zeta)}\, d\zeta\, \delta(\omega - n\Omega) \qquad \text{(A1)}$$

where

$$f_n(\zeta) = k\left(k\zeta L - \frac{nD}{a}\right)[J_n(ka\gamma) + A_n(k\gamma)]\sqrt{\frac{2}{\pi\gamma k r_0}} \times \exp[in(\phi_0 - \pi/2) - i\pi/4]$$

with $\zeta = \alpha/k$, and $\gamma = \beta/k = \sqrt{1-\zeta^2}$. It has also been necessary to use the relationship

$$J_{|n|}(x)e^{i|n|\pi/2} = J_n(x)\, e^{in\pi/2}$$

The phase term that depends on the observer location has been reduced as

$$\beta r_0 + \alpha z_0 = kR_0(\gamma \sin\theta_0 + \zeta \cos\theta_0) = kR_0\phi_e(\zeta)$$

where $r_0 = R_0 \sin\theta_0$ and $z_0 = R_0 \cos\theta_0$. In the limit $kR_0 \gg 1$, the integral or Eq. (A1) may be evaluated using the method of stationary phase.

Stationary phase points occur when $\phi_e'(\zeta) = 0$, and since $0 < \theta_0 < \pi$, there will be only a single stationary point that occurs when $\zeta = \cos\theta_0$. The integral in Eq. (A1) is then approximated as

$$\int_{-\infty}^{\infty} f_n(\zeta)e^{ikR_0\phi_e(\zeta)}\, d\zeta = f_n(\cos\theta_0)\sqrt{\frac{2\pi}{kR_0|\phi_e''|}}\, e^{ikR_0\phi_e(\cos\theta_0) + i\mu\pi/4}$$

where $\mu = \text{sgn}(\phi_e'')$. Since $\phi_e''(\cos\theta_0) = -1/\sin^2\theta_0$, it follows that the left-hand side of this equation becomes

$$-i\left(kL\cos\theta_0 - \frac{nD}{a}\right)[J_n(ka\sin\theta_0) + A_n(k\sin\theta_0)] \times \frac{2}{R_0}\, e^{ikR_0 + in(\phi_0 - \pi/2)}$$

which, when substituted into Eq. (A1), with $n = mB$ and $k = mB\Omega/c_0$, gives Eq. (5). In this Appendix, mB has been replaced by n, and so the same analysis may also be applied to the unsteady load formulation.

Acknowledgment

This work was supported by NASA Grant NAG-1-715.

References

[1]Gutin, L., "On the Sound of a Rotating Airscrew," NACA TM 1195, 1948.

[2]Lowson, M. V., and Ollerhead, J. B., "A Theoretical Study of Helicopter Rotor Noise," *Journal of Sound and Vibration,* Vol. 9, 1969, pp. 197–222.

[3]Farassat, F., "The Prediction of the Noise of Supersonic Propellers in the Time Domain—New Theoretical Results," AIAA Paper 83-0743, Jan. 1983.

[4]Hanson, D. B., "Noise of Counter-Rotation Propellers," *Journal of Aircraft,* Vol. 22, No. 7, 1985, pp. 609–617.

[5]Goldstein, M. E., *Aeroacoustics,* McGraw-Hill, New York, 1976.

[6]James, J. H., "Far-Field Sound Radiation of Point Sources Near Locally Reacting Cylinder," AMTE Tech. Memo TM81036, March 1981.

[7]Fuller, C. R., "Free Field Correction Factor for Spherical Acoustic Waves Impinging on Cylinders," *AIAA Journal,* Vol. 27, No. 12, 1989, pp. 1722–1726.